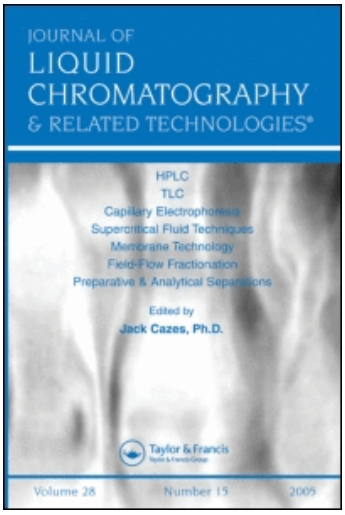

Journal of Liquid Chromatography & Related Technologies
Publication details, including instructions for authors and subscription information:
http://www.informaworld.com/smpp/title~content=t713597273

On the Concentration Effects in Micro-Thermal Field-Flow Fractionation of Polymers

Josef Janča[a]; Irina A. Ananieva[b]
[a] Université de La Rochelle, Pôle Sciences et Technologie, La Rochelle Cedex, France [b] Chemistry Department, Lomonosov Moscow State University, Moscow, Russia

To cite this Article Janča, Josef and Ananieva, Irina A.(2008) 'On the Concentration Effects in Micro-Thermal Field-Flow Fractionation of Polymers', Journal of Liquid Chromatography & Related Technologies, 31: 18, 2721 — 2736
To link to this Article: DOI: 10.1080/10826070802388086
URL: http://dx.doi.org/10.1080/10826070802388086

Journal of Liquid Chromatography & Related Technologies®, 31: 2721–2736, 2008

ISSN: 1082-6076 print/1520-572X online
DOI: 10.1080/10826070802388086

On the Concentration Effects in Micro-Thermal Field-Flow Fractionation of Polymers

Josef Janča[1] and Irina A. Ananieva[2]

[1]Université de La Rochelle, Pôle Sciences et Technologie, La Rochelle Cedex, France
[2]Lomonosov Moscow State University, Chemistry Department, Moscow, Russia

Abstract: Micro-Thermal Field-Flow Fractionation (Micro-TFFF) was used to study the effect of concentration of the polymer solutions injected into the separation channel. The range of the investigated concentrations was very large, becoming higher then the critical values at which the entanglement of the polymer coils leads to the formation of the macromolecular aggregates. The samples of different molar masses were used and the experiments were carried out at different temperature drops across the channel and at different temperatures of the cold wall. The multiple peaks (or oscillations) that appeared on the fractograms at a given concentration of the injected sample solution and at a given temperature drop, disappeared at lower concentration and emerged again at the same lower concentration, but at a higher temperature drop. Although the observed broadening of the fractograms can be partially caused by the formation of the macromolecular aggregates, their presence cannot explain the secondary peaks or oscillations appearing on the fractograms at the retentions corresponding to extremely high molar masses. The hydrodynamic and/or gravitational instabilities, which are caused by the formed viscosity and density gradients inside the separation channel are the most probable explanation of the origin of the mentioned secondary peaks and/or oscillations emerging at high concentrations and/or high temperature drops.

Correspondence: Josef Janča, Université de La Rochelle, Pôle Sciences et Technologie, Avenue Michel Crépeau, La Rochelle Cedex 01, France 17042. E-mail: jjanca@univ-lr.fr

Keywords: Concentration effects, Hydrodynamic instabilities, Intrinsic viscosities at extreme temperatures, Micro-Thermal Field-Flow Fractionation, Viscosity effects

INTRODUCTION

The effect of the injected amount of polymer solution and of its concentration on the retention, zone width, and on the whole elution profile reflected in the shape of the fractogram in Thermal Field-Flow Fractionation (TFFF) was already investigated. The most complete study of this problem was published by Caldwell et al.[1] We have studied the effect of concentration in Micro-TFFF with the use of ultra-high molar mass (UHMM) polymers.[2,3] Although the experimental results found by different authors agree quite well, there are some differences concerning the interpretation of the experimental observations. From the analytical viewpoint, it is sufficient to optimize the experimental conditions in order to suppress the effect of the concentration, or to minimize it, so that the molar mass distribution of the investigated polymer sample is determined correctly. On the other hand, the full understanding of the origin of concentration effects is important whenever any auxiliary phenomena are studied, such as solution behavior of the UHMM polymers, the possible chain degradation, the emergence of the hydrodynamic instabilities under the conditions of Micro-TFFF, etc.

Our previous experience with the effect of concentration, published in several papers concerned the separations of the polymers by Size-Exclusion Chromatography (SEC)[4–8] and it was reproduced later by some authors in the studies of the separations in liquid chromatography. This experience inspired the idea[9] that the dominant contribution to the shift of the retention volume and perturbation of the elution profile is due to viscosity gradients and consequent hydrodynamic effects like Rayleigh-Taylor gravitational instability or Saffman-Taylor instability (viscous fingering effect). Later on, Ligrani et al.[10] and Gupta et al.[11] studied the numerical modeling and experimental flow instabilities from unstable stratification of density in the channel shear layers at low Reynolds numbers; they found that the above mentioned instabilities actually exist under the investigated experimental conditions. Our explanation[9] of the peculiar shape of the elution profiles at high concentrations was, thus, supported. Contado et al.[12] studied, experimentally, the effect of concentration of polystyrene in decaline on the Soret coefficient $S_T = D_T/D$, where D_T is the coefficient of thermal diffusion and D is the diffusion coefficient. They have found that the retention time, the value of S_T, the width, and distortion of the peaks increase with increasing sample concentration, the more so as the cold wall

temperature is lower and molar mass of the polymer higher. Martin and Feuillebois[13] studied, theoretically, the effect of the concentration on the retention in FFF, compared their results with the published experimental data, and concluded that the observed increase in average retention of the species behaving as random coils is caused by the viscosity effects. The above mentioned findings agree with our original idea[9] that viscosity gradients formed inside the channel and the consequent hydrodynamic instabilities represent the most important contribution to the concentration effect.

EXPERIMENTAL

The apparatus for Micro-TFFF used in this work consisted of a syringe pump model IPC 2050 (Linet Compact, Czech Republic), equipped with a 20 mL precision stainless steel syringe (Institute of Scientific Instruments, Academy of Sciences, Czech Republic), an injection valve model 7410 (Rheodyne, USA) with a 1 μL loop, a UV-VIS variable wavelength detector model UV-975 (Jasco, Japan) equipped with the 1 μL cell, and an integrator Model HP 3395 (Hewlett-Packard, USA).

The versatile Micro-TFFF channel model MicroFrac Compact was developed in our laboratory and is commercially available. The dimensions of the micro-channel used in this work were $0.1 \times 3.2 \times 72$ mm. The cold wall temperature was controlled and kept constant by using a compact, low temperature thermostat model RML 6 B (Lauda, Germany). The electric power for the heating cartridge was regulated by an electronic device constructed in our laboratory and is also commercially available. The temperatures of the cold and hot walls were measured by digital thermometer (Hanna Instruments, Portugal) equipped with two thermocouples.

The apparatus for SEC consisted of a reciprocal pump model L6000 (Merck, Germany), an injection valve model 7125 (Rheodyne, USA) with a 20 μL loop, a separation column TSK Gel 7.8 I.D. × 30 cm, a UV-VIS variable wavelength detector model L4000 (Merck, Germany) equipped with the 10 μL cell, and an integrator model HP 3395 (Hewlett-Packard, USA).

A standard Ubbelohde capillary viscometer with model AVS 410 (Schott, Germany) automatic viscometer was used to determine the variation of the intrinsic viscosity of one polystyrene (PS) standard with the temperature.

The tetrahydrofuran (THF) for HPLC (Carlo Erba, Italy) was used as a carrier liquid in Micro-TFFF, SEC, and for viscometry measurements. The PS standards of different molar masses (various suppliers)

Table 1. Molar masses of polystyrene standards

Polystyrene Standard	M_w (g/mol)	M_n (g/mol)	M_w/M_n	M_w (g/mol)
	Supplier's data			SEC Corrected
PS 115	115 000	Not given	<1.04	120 000
PS 630	630 000	Not given	<1.11	550 000
PS 675	675 000	Not given	<1.10	679 000
PS 1030	1 030 000	Not given	<1.06	990 000

were used in this study. Their molar masses provided by the suppliers are given in Table 1.

RESULTS AND DISCUSSION

Molar Masses of the Studied Polymers

A detailed analysis of the origin of concentration effects necessitates the determination of the accurate average molar masses of the investigated polymer samples. The accuracy of such data is limited by the precision of the light scattering and osmometry methods used frequently for the determination of average molar masses. Although SEC is only a separation method, it provides more repeatable, reproducible, and thus precise results in comparison with the mentioned methods of average molar mass determination. Consequently, the SEC can conveniently be used as an independent method to check the accuracy and consistency of the average molar masses of the studied PS standards. However, the calibration curve has to be determined by using several standards in order to correct the average molar masses of the samples whose points do not lie on the calibration curve within the range of SEC experimental errors. The results are in Figure 1, which shows the calibration curve of the SEC column constructed by using 22 PS standards of different molar masses. Most of the experimental points in Figure 1 fit well with the presumed linear central part of the calibration plot. However, some of them lie repeatedly above or below the calibration straight line and these deviations are out of the limits of experimental errors of the SEC. The repeatability of the retention times determined by several injections of some of the PS samples used for the construction of the calibration plot was better than 0.02 min within the whole range of the molar masses. As a result, the molar masses of these systematically deviating PS standards were corrected according to the SEC results by using the calibration plot in Figure 1 and the corresponding retentions. The corrected, as well as, original average molar masses are given in Table 1. The PS standards

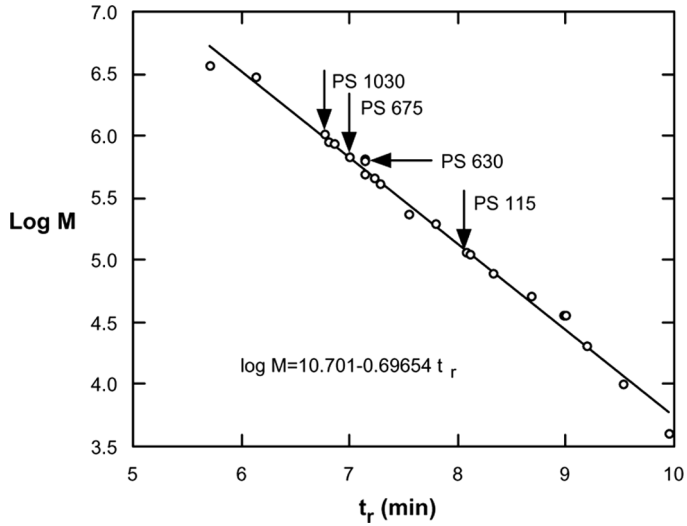

Figure 1. Calibration curve of the SEC column. The arrows indicate the PS standard chosen for further study.

chosen for further investigation and covering an extended molar mass range from 115,000 to 1,030, 000 g/mol are indicated by the arrows in Figure 1.

Viscosities of the Studied Polymer Solutions

Our previous studies[2,3] indicated that the viscosity gradient formed within the zone of the retained macromolecules can be one of the important factors leading to the perturbation of the shape of the fractograms, which appears whenever relatively concentrated polymer solutions are injected. Moreover, it has been shown that an increase of the retention amplifies the concentration effect.[3] Consequently, the specific viscosity η_{sp} of a polymer solution at a given concentration and temperature must be known. It can be calculated from Huggins equation:

$$\eta_{sp}/c = [\eta] + k_H[\eta]^2 c \tag{1}$$

where c is the concentration and k_H is empirical Huggins constant valid for a given polymer solvent system. The intrinsic viscosity $[\eta]$ can be measured according to the definition of this parameter:

$$[\eta] = \lim_{c \to 0}(\eta_{sp}/c) \tag{2}$$

by extrapolating the concentration dependence η_{sp}/c versus c to zero concentration. The specific viscosity η_{sp} can be calculated from the relative viscosity η_{rel}:

$$\eta_{sp} = \eta_{rel} - 1 \tag{3}$$

which is defined as the ratio of the viscosity of a polymer solution to the viscosity of the pure solvent at the same temperature. The intrinsic viscosity $[\eta]$ is related to the molar mass M of a polymer dissolved in a solvent at a given temperature by Mark-Houwink equation:

$$[\eta] = KM^a \tag{4}$$

where K and a are the constant and exponent determined experimentally by correlating $[\eta]$ and M values for several samples of different molar masses.

Since the variation of the retention and shape of the factogram in Micro-TFFF is supposed to be a consequence of the formation of viscosity and density gradients at different temperatures inside the channel, it is evident that the solution viscosity behavior of the studied PS standards must be known within the relevant temperature range. The complication is that most of the published data[14] concerning the above mentioned Huggins and Mark-Houwink equations were obtained at one temperature only (usually 25°C) or, in the best cases, within a relatively restricted temperature range. As a result, in order to interpret accurately the experimental data from Micro-TFFF, it was necessary to determine the required parameters of the Huggins and Mark-Houwink equations experimentally within an extended range of temperature.

However, not only the temperature dependence of the viscosity of the studied PS standard solutions must be determined but also the temperature dependence of the viscosity of the THF used as solvent and carrier liquid. Some data concerning this dependence were found in the literature,[15–18] but we have performed the viscometry measurements of the temperature dependence of the THF in order to check the accuracy and consistency of the published data as well as that of our viscometry determination of the parameters of the Huggins and Mark-Houwink equations.

The dependence of the density ρ of THF on the temperature, necessary for the calculation of the viscosity μ from the experimental kinematic viscosities ν defined according to:[19]

$$\mu = \rho \times \nu \tag{5}$$

was not found in the literature. Our experimental data obtained by weighing a known volume of THF taken at the given temperature are

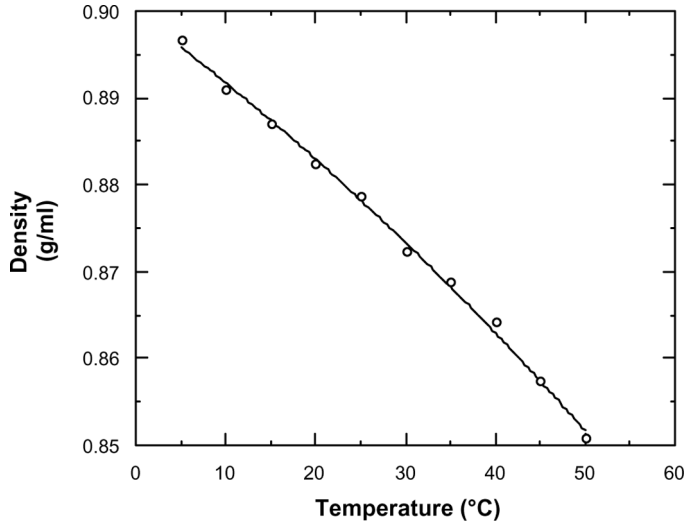

Figure 2. Dependence of the density (g/mL) of tetrahydrofurane on the temperature.

shown in Figure 2. The dependence of the density of THF on the temperature (in °C) calculated from our experimental data is approximated by the relationship:

$$\rho = 0.8997 - 0.0007558 \times T - 4.091 * 10^{-6} \times T^2 \qquad (6)$$

obtained by the linear regression of the experimental data. The regression coefficient $R = 0.9985$ indicates very good precision of the density measurements.

The accuracy of the viscometry measurements was verified also by the comparison of our experimentally determined temperature dependence of the viscosity of pure water with that found in the literature.[15,16] The dependence of the density of water on the temperature was taken from the references.[15,16] The results of the viscometry measurements of the pure THF and water are in Figure 3, which demonstrates that our experimental points concerning the viscosity of water fit perfectly with the literature data,[15,16] and the agreement of our experimental and published viscosities[15] of THF is also very good. Unfortunately, some other proposed relationships[17,18] do not fit at all with our experimental or literature data represented in Figure 3.

Some plots η_{sp}/c versus c allowing the determination of the intrinsic viscosity of the PS 630 (corrected molar mass 595 000 g/mol) in THF at various temperatures are shown in Figure 4. Fair linearity of these plots

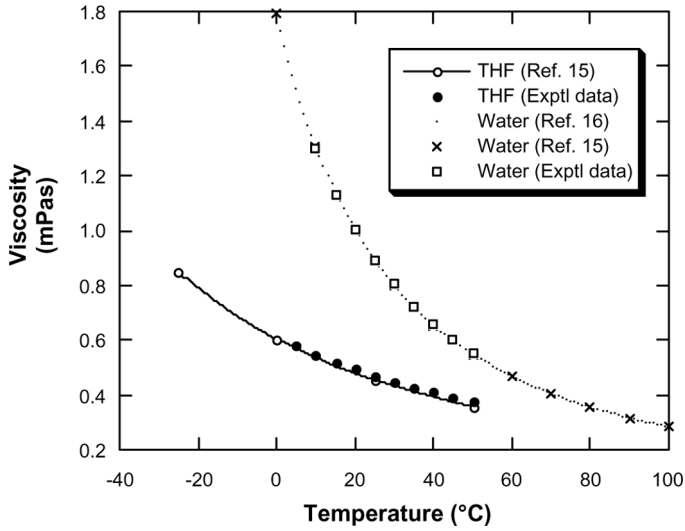

Figure 3. Comparison of the dependences of the viscosity of tetrahydrofurane and water measured experimentally in this work and found in the literature.

indicates that the range of the concentrations lies well in the dilute solution regime. All viscometry data were used to determine the dependence of the intrinsic viscosity on the temperature within the temperature range from −10°C to 50°C and Huggins constants at the appropriate temperatures. As a matter of fact, this temperature range is more extended in

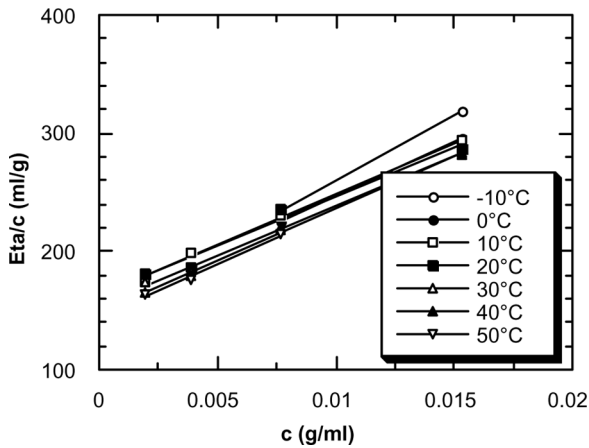

Figure 4. Plots of η_{sp}/c as a function of the concentration of PS 630 measured in tetrahydrofurane at different temperatures. The intrinsic viscosities were calculated from these plots as indicated in the text.

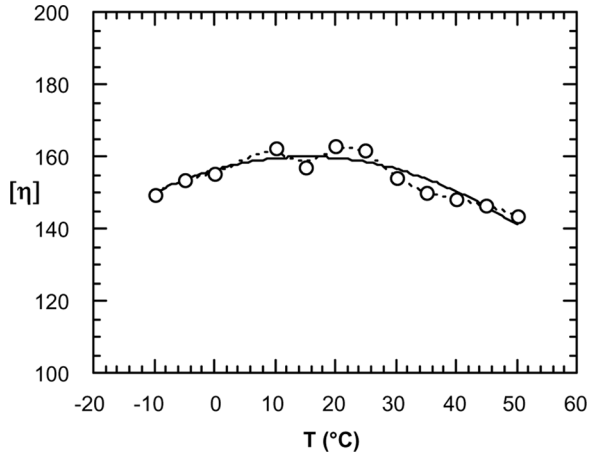

Figure 5. Dependence of the intrinsic viscosity [η] of PS 630 in tetrahydrofurane on the temperature.

comparison with that applied in the present Micro-TFFF experiments, but the data will be used in our future studies and might be also of general interest. The dependence of [η] versus T is demonstrated in Figure 5 and the corresponding Huggins constant are given in Table 2.

The variation of the intrinsic viscosity with the temperature in Figure 5 reflects the variation of the effective hydrodynamic volume of the polymer chains in solution. Since this variation is not monotonous but exhibits a maximum around the temperature 20°C (or perhaps two local maxima at 10°C and 20°C, see the dashed curve in Figure 5), at least two molecular mechanisms can be considered. A change of the solvatation of the polymer chains by the solvent molecules and a change of intra-molecular mobility of the polymer chains both vary with the temperature. The intra-molecular mobility increases, in general, with increasing temperature and the polymer coils in solution are more expanded. On the other hand, the interactions of the solvent molecules with the polymer chains and, thus, the solvatation and swelling of the coils can exhibit more complex behavior with varying temperature. As a result, the observed dependence of the intrinsic viscosity of the studied PS sample on the temperature with a notable maximum can be explained by a

Table 2. Huggins constants calculated from the viscometry data

T (°C)	5	10	15	20	25	30	35	40	45	50
k_H	0.34	0.33	0.36	0.31	0.31	0.35	0.38	0.40	0.42	0.44

coupled and complex action of each of the mentioned molecular mechanisms. The viscometry study was carried out by using only one PS 630 standard. The reason was that the consumption of the expensive sample is high for such an extensive investigation. However, solution behavior of linear PS standards in THF at one temperature (25°C) was studied previously.[20] The Mark-Houwink equation, valid for linear PS in THF at 25°C, was determined on the basis of the experimental data and of the data found in the literature. The resulting Mark-Houwink equation is:[20]

$$[\eta] = 1.17 \times 10^{-2} M^{0.717} \tag{7}$$

for the intrinsic viscosity $[\eta]$ expressed in mL/g and concentrations c in g/mL. The Huggins constant was found[14] as only slightly varying from 0.364 to 0.367 within the relevant molar mass range. These data and the dependence of the intrinsic viscosity and of the Huggins constant on the temperature determined for reference PS 630 standard were, thus, used to calculate the specific viscosities at different temperatures of other samples by supposing that it is reasonable to expect that the solution behavior of linear PS standards is independent of the molar mass within the investigated molar mass range.

The consitency of our SEC and viscometry data was confirmed by calculating the intrinsic viscosity of the PS 630 standard with the use of its corrected molar mass $M = 550{,}000$ g/mol and of the Mark-Houwink Equation (7). The calculated value $[\eta\ ]_{\text{calc}} = 155$ mL/g is in good agreement with the experimental value $[\eta]_{\text{exp}} = 161$ mL/g obtained by the viscometry at 25°C.

Critical Concentration of the Studied Polymer Solutions

The secondary peaks occurring at higher concentrations of the injected polymer solutions were attributed previously[1] to relatively stable aggregates or microgels, formed already in stock polymer solution whose concentration was above the critical one. Under such conditions, the macromolecular chains become entangled. Nevertheless, our recent study[3] indicated that a secondary peak, absent at lower retention of the studied polymer sample, reappears if the same sample injected at the same concentration is retained more due to a higher temperature drop. This finding makes improbable the explanation of the secondary peak by a presence of stable aggregates in the stock solution. Although a temporary entanglement of the chains inside the channel cannot be excluded, it is not understandable why such structures should not disaggregate when they leave the eluting zone (due to their higher retention in comparison with the individual chains) and, thus, become more diluted

by dispersive processes. Moreover, it is difficult to associate the oscillatory shape of the fractograms with the presumed monotonous molar mass distribution (MMD) of the retained macromolecules containing some portion of the entangled chains. Even if the aggregates are composed by the longest polymer chains, the formation of stable aggregates of very high apparent molar masses corresponding to at least five to ten single chains[3] is not very probable under the conditions of Micro-TFFF experiments. Consequently, a deeper investigation of the impact of the concentration (above the critical one) on the shape of the fractogram makes up part of this study.

The critical concentration c^* (in g/g of the solution) can be calculated from:

$$c^* = M/(N_A \rho \langle r \rangle^3) \tag{8}$$

where N_A is Avogadro number, ρ is the density of the solvent in g/mL, and $<r>$ is the radius of gyration. A combination of the Equation (8) with an empirical relationship relating $<r>$ with the M:

$$\langle r \rangle = 1.45 \times 10^{-9} M^{0.595} \tag{9}$$

found in the literature[21] and valid for PS in thermodynamically good solvent, results in:

$$c^* = 545 \rho^{-1} M^{-0.785} \tag{10}$$

We suppose that viscosity gradients formed in the eluting zone represent the major factor generating the oscillations on the elution profiles at high concentrations. The specific viscosity η_{sp}^* of the solution at the critical concentration c^* can thus be calculated by combining Equations (1) and (10).

Effect of Concentration on Micro-TFFF Fractograms

The experimental conditions of Micro-TFFF were chosen to allow the identification of different contributions to the concentration effect. The flow rate was low and identical in all experiments (10 μL/min). The initial concentrations of all polymer solutions, independently of the molar mass of the concerned PS standard, were all approximately 2.5 times higher than the critical concentration c^* and adjusted so as the specific viscosities of all solutions were equal. The diluted solutions were prepared from the initial ones by consecutive dilutions by a factor 2. The results of the experiments are shown in Figures 6 to 9.

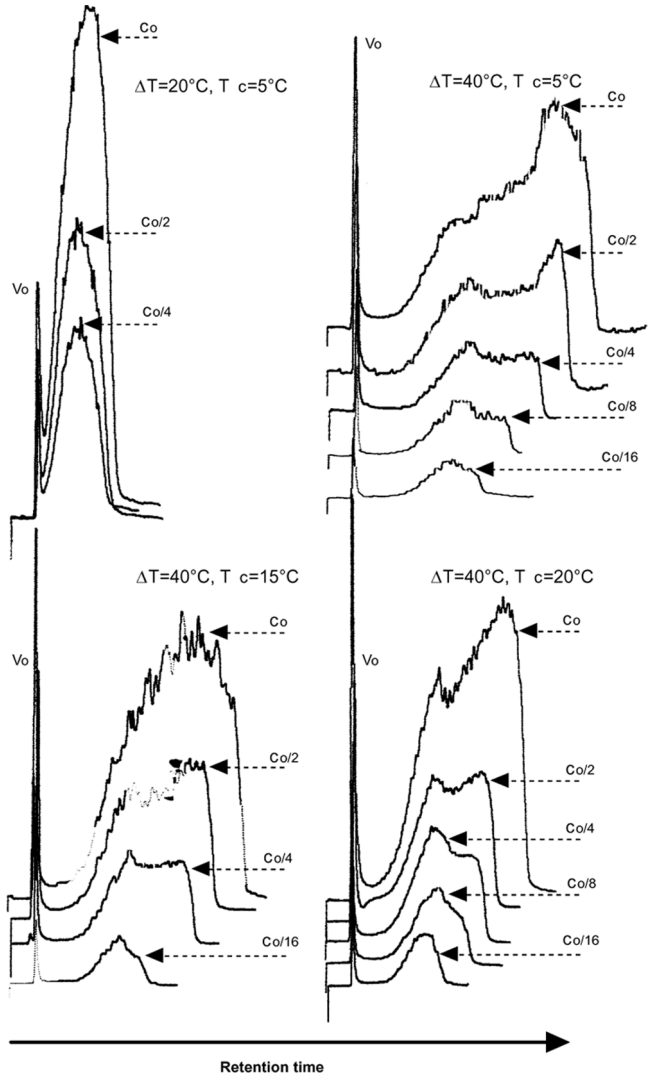

Figure 6. Effect of concentration of PS 630 on the shape of the fractograms at different temperature drops and different temperatures of the cold wall.

Figure 6 demonstrates how the temperature of the cold wall T_c and temperature drop ΔT influence the shape of the fractograms at different concentrations. An increase of ΔT from 10°C to 40°C at the same $T_c = 5$°C causes a dramatic change of the fractogram shape and the appearance of the secondary peaks. Although at low ΔT and, thus, at low retention, the secondary peaks do not appear even at the highest initial concentration c_0,

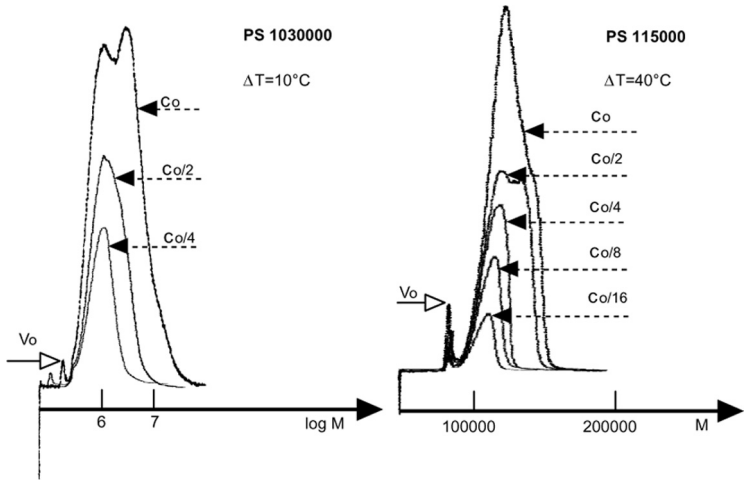

Figure 7. Effect of concentration on the shape of the fractograms of PS 1,030,000 and PS 115 at the same temperature of the cold wall $T_c = 10°C$ and different temperature drops. ΔT chosen so that the retentions of both samples are approximately the same.

which is largely above c^* from the very beginning; the secondary peak disappears only at the lowest concentrations independently of T_c. This result indicates that the most important contribution to the effect of concentration is due to the formation of strong viscosity and density gradients and the resulting occurrence of the mentioned hydrodynamic instabilities. However, the formation of the macromolecular aggregates due to the entanglement of the chains at high concentrations cannot be excluded.

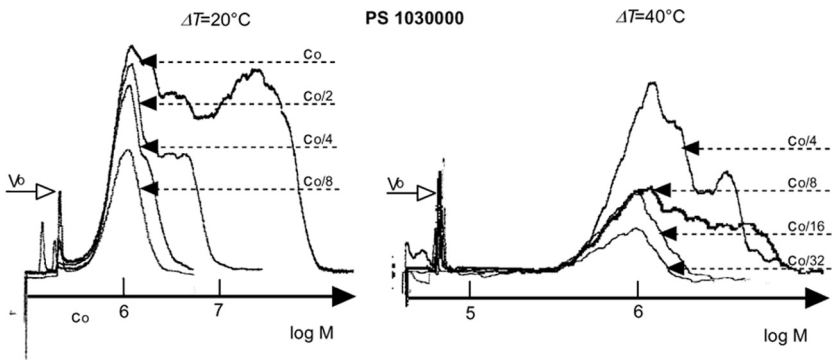

Figure 8. Effect of concentration and higher temperature drops ΔT on the shape of the fractograms of PS 1,030,000 at the same temperature of the cold wall $T_c = 10°C$.

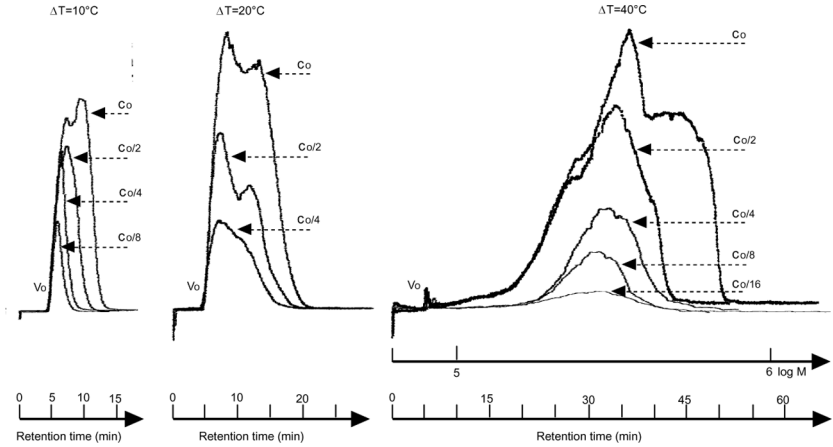

Figure 9. Effect of concentration of PS 675 on the shape of the fractograms at different temperature drops and identical temperatures of the cold wall $T_c = 11°C$.

Figure 7 demonstrates that the solutions of two polymers of very different molar masses injected into the channel at different concentrations, but adjusted so that the initial specific viscosities are the same, and exposed to different ΔT, but chosen so the retentions of both samples are practically identical, exhibit very small differences in the shapes of the resulting fractograms. Slightly broader fractograms of the high molar mass sample are probably due to higher polydispersity, but it may result also from a lower diffusion coefficient. In Figure 8, can be seen what happens when the retention of the high molar mass sample increases due to an increase in ΔT. This behavior, together with the observation that the position of the secondary peak or tailing on the fractograms of the low molar mass sample does not correspond to an important increase of the molar mass (see the scale of molar masses), indicates that the contribution of the viscosity gradient and of the resulting hydrodynamic instabilities is more important than the aggregation by the entanglement of the macromolecular chains in solution at high concentration. Even if the entanglement of the chains exits near the accumulation wall, it should be reversible due to the thermal motion of the polymer chain segments and should disappear during the elution by progressive dilution of the sample. It is also obvious that the dilution of the zone during the elution causes the decrease of the concentration below the critical value c^* much sooner, in comparison with the disappearance of the important concentration gradients leading to hydrodynamic instabilities. This fact also supports the hypothesis of dominant viscosity gradient phenomena.

Figure 9 represents the evolution of the shape of the fractograms of the sample of polystyrene of medium molar mass as a function of the concentration and retention. It has to be stressed, that the concentrations of the injected polymer solutions are below the critical values c^* only starting with $c_0/4$ and lower. On the low retention extreme, at lowest ΔT, the position of the peak maxima progressively shifts to lower retention times with the decreasing concentration and the secondary peak is distinguishable only at the highest concentration. On the high retention extreme, at highest ΔT, the peaks are much larger, and they exhibit the oscillations (secondary peaks); this behavior totally disappears only at the lowest concentration of the injected solution. This observation represents an additional proof of the dominancy of the hydrodynamic instabilities in overall concentration effects.

One of the conclusions of our previous study,[3] dealing with the investigation of the stability of UHMM polymers with respect to a possible shear degradation under the conditions of Micro-TFFF, was that the oscillating shape of the fractogram is well repeatable under the identical experimental conditions. This former conclusion[3] was confirmed by the present more detailed investigation. The reproducibility of the concentration effects is evidenced by the fact that different authors cited in this paper have observed the same behavior. The only difference in comparison with the present results is that the oscillation or "infrastructure" of the fractograms obtained in this and previous studies[3] is much finer, which is due to relatively slow linear velocities of the carrier liquid. Consequently, the "fingerprint" of the hydrodynamic instabilities is exhibited with an increased "resolution".

CONCLUSION

Our experimental study contributed to the understanding of the origin of concentration effects. It has definitely been confirmed that the most important factor, which produces the shift of the retention and the occurrence of the oscillations on the elution profiles at high concentrations of the injected polymers samples is the formation of the hydrodynamic instabilities due to the formed viscosity and density gradients. However, from the practical point of view, it is preferable to perform the Micro-TFFF experiments at as low as possible concentrations, which facilitate the quantitative interpretation of the fractograms and data treatment.

REFERENCES

1. Caldwell, K.D.; Brimhall, S.L.; Gao, Y.; Giddings, J.C. J. Appl. Polym. Sci. **1988**, *36*, 703.
2. Janča, J. J. Liq. Chromatogr. & Rel. Technol. **2002**, *25*, 683.

3. Janča, J.; Strnad, P. J. Liq. Chromatogr. & Rel. Technol. **2004**, *27*, 187.
4. Janča, J. J. Chromatogr. **1977**, *134*, 263.
5. Janča, J.; Pokorný, S. J. Chromatogr. **1978**, *148*, 31.
6. Janča, J. J. Chromatogr. **1979**, *170*, 309.
7. Janča, J.; Pokorný, S. J. Chromatogr. **1979**, *170*, 319.
8. Janča, J. Anal. Chem. **1979**, *51*, 637.
9. Janča, J.; Martin, M. Chromatographia **1992**, *34*, 125.
10. Ligrani, P.L.; Gupta, S.; Giddings, J.C. Int. J. Heat Mass Transfer **1998**, *41*, 1667.
11. Gupta, S.; Ligrani, P.L.; Giddings, J.C. Int. J. Heat Mass Transfer **1999**, *42*, 1023.
12. Contado, C.; Martin, M.; Dondi, F.; Melucci, D. Chromatographia **2002**, *56*, 495.
13. Martin, M.; Feuillebois, F. J. Sep. Sci. **2003**, *26*, 471.
14. *Polymer Handbook,* 3rd Ed.; Brandrup, J. Immergut, E.H., Eds.; Wiley: New York, 1989.
15. *Handbook of Chemistry and Physics,* 83rd Ed.; Lide, D.R., Ed.; CRC Press: Boca Raton, 2002–2003.
16. *Kratkij Spravochnik po Khimii,* 3rd Ed.; Kurilenko, O.D., Ed.; Naukovaya Dumka: Kiev, 1965.
17. Belgaeid, J.E.; Hoyos, M.; Martin, M. J. Chromatogr. A. **1994**, *678*, 85–96.
18. Regazetti, A.; PhD. Thesis, N° O2AIX30019, Université d'Aix-Marseille III, France, 2002.
19. Bird, R.B.; Stewart, W.E.; Lightfoot, E.N. *Transport Phenomena*, Wiley and Sons, Inc.: New York, 1960.
20. Kolínský, M.; Janča, J. J. Polym. Sci., Polym. Chem. Ed. **1974**, *12*, 1181.
21. Adam, M.; Delsanti, M. Macromolecules **1977**, *10*, 1229.

Received February 14, 2008
Accepted February 22, 2008
Manuscript 6325